Summertime formaldehyde observations in New York City: Ambient levels, sources and its contribution to HOx radicals

Yu Chi Lin,[1,2] James J. Schwab,[1] Kenneth L. Demerjian,[1] Min-Suk Bae,[1,3] Wei-Nai Chen,[1,2] Yele Sun,[4] Qi Zhang,[5] Hui-Ming Hung,[6] and Jacqueline Perry[7]

Received 3 July 2011; revised 15 March 2012; accepted 16 March 2012; published 26 April 2012.

[1] Measurements of ambient formaldehyde (HCHO), related gases and particulate matter were carried out from the SUNY Albany mobile platform at the Queens College site in New York City (NYC) from 15 July to 3 August 2009. Ambient HCHO was measured using a quantum cascade laser (QCL) trace gas detector. HCHO concentrations ranged from 0.4 to 7.5 ppb with a mean value of 2.2 ± 1.1 ppb. Daily HCHO peaks were nearly always found between 1100 EST (Eastern Standard Time) and noontime throughout the sampling period. HCHO correlated strongly with NOx and black carbon during the traffic rush hours, but around noontime HCHO correlated much better with total oxidants ($Ox = O_3 + NO_2$). Using the diurnal pattern of HCHO/BC ratios, we estimated that 70% of HCHO present between 1200 EST to 1500 EST was produced by photochemical reactions. Sources of photochemically produced HCHO were calculated using measured concentrations of hydrocarbons, their reaction kinetics with OH radicals, and HCHO yields. These calculations indicated that isoprene oxidation was the dominant source of HCHO for this period at this site, responsible for 44%, followed by methane (25%) and propene (18%). To assess the impact of HCHO as a radical source, the HOx production rates from HCHO, HONO, O_3 photolysis, and alkenes $+O_3$ were calculated as well. Daily averaged HOx production rates from HONO, HCHO, O_3 photolysis and alkenes $+O_3$ were 8.6×10^6, 2.3×10^6, 1.7×10^6, 2.1×10^5 molecules cm^{-3} s^{-1}, respectively, contributing 67, 18, 13 and 2% to the overall daily HOx radical budget from these precursors.

Citation: Lin, Y. C., J. J. Schwab, K. L. Demerjian, M.-S. Bae, W.-N. Chen, Y. Sun, Q. Zhang, H.-M. Hung, and J. Perry (2012), Summertime formaldehyde observations in New York City: Ambient levels, sources and its contribution to HOx radicals, *J. Geophys. Res.*, *117*, D08305, doi:10.1029/2011JD016504.

1. Introduction

[2] Formaldehyde (HCHO) is the simplest, most important and abundant carbonyl compound in the atmosphere. HCHO is a ubiquitous component due to its sources from photochemical-oxidation processes, but it is often present at low levels due to its short lifetime against removal via photolysis and further oxidation. In urban areas, primary emissions from combustion sources can be a major contributor to ambient HCHO [*Anderson et al.*, 1996; *Kolb et al.*, 2004; *Dasgupta et al.*, 2005; *Herndon et al.*, 2005; *Li et al.*, 2010; *Rappenglück et al.*, 2010]. *Anderson et al.* [1996] found that in Denver the HCHO peak was always observed before noontime, suggesting the importance of motor vehicle sources in their study. *Dasgupta et al.* [2005] showed that the nighttime HCHO peak observed in Atlanta coincided with a CO peak, again indicating that motor vehicle emissions were a major source of ambient HCHO. During vehicle "chasing" experiments conducted with the Aerodyne Mobile Laboratory, *Herndon et al.* [2005] found that HCHO emission ratios from in-use compressed natural gas (CNG) buses were approximately 15 times higher than those from diesel-powered buses, suggesting that CNG vehicles have the potential to be an important source of HCHO in New York City (NYC). In more work with the Aerodyne Mobile Laboratory, *Kolb et al.* [2004] indicated a good correlation between HCHO and CO_2 on the roadside in cool and cloudy mornings in Mexico City, deducing that HCHO mainly came from mobile sources on cloudy days.

[3] While primary emissions have been shown to be an important contributor to ambient HCHO in urban areas, the oxidation of volatile organic carbon is also responsible for

[1]Atmospheric Sciences Research Center, State University of New York at Albany, Albany, New York, USA.
[2]Research Center for Environmental Changes, Academia Sinica, Taipei, Taiwan.
[3]Department of Environmental Engineering, Mokpo National University, Muan, South Korea.
[4]State Key Laboratory of Atmospheric Boundary Layer Physics and Atmospheric Chemistry, Institute of Atmospheric Physics, Chinese Academy of Sciences, Beijing, China.
[5]Department of Environmental Toxicology, University of California, Davis, California, USA.
[6]Department of Atmospheric Sciences, National Taiwan University, Taipei, Taiwan.
[7]New York State Department of Environmental Conservation, Albany, New York, USA.

0148-0227/12/2011JD016504

secondary HCHO production, particularly under strong radiation conditions. *Satsumabayashi et al.* [1995] utilized the nighttime ratio of HCHO/CO to assess the amount of secondary HCHO in central Japan. They proposed that 53% of formaldehyde was produced by photochemical reactions at Urawa. In downtown Mexico City, the primary and secondary HCHO were partitioned using a linear regression model, suggesting that primary and secondary HCHO accounted for approximately 40 and 42% of total ambient HCHO, respectively, while the residual 18% was explained by the background level, which possibly originated from both sources [*Garcia et al.*, 2006].

[4] Secondary HCHO is a product of the oxidation of a large array of volatile organic compounds (VOCs), both anthropogenic and biogenic. In particular, terminal alkenes such as isoprene (C_5H_8), ethene (C_2H_4) and propene (C_3H_6) react with OH radical to form HCHO and HO_2:

$$(R1) \quad >C=CH_2 + OH \rightarrow +(O_2, NO) \rightarrow >C\cdot + HCHO + HO_2\cdot$$

[5] One major channel in the photolysis of HCHO leads to the formation of HO_2-radicals, which react with NO, rapidly converting to OH radicals via reactions R3 to R4.

$$(R2) \qquad HCHO + h\nu \rightarrow H_2 + CO; \ \lambda \leq 360 \text{ nm}$$

$$(R3) \quad HCHO + h\nu \rightarrow H + CHO(+2O_2) \rightarrow 2HO_2\cdot + CO; \lambda \leq 335 \text{ nm}$$

$$(R4) \qquad HO_2 + NO \rightarrow OH\cdot + NO_2.$$

[6] In Rome, the HOx (OH + HO_2) production rate from HCHO was 1×10^6 molecules/ cm^3/s, which was one order of magnitude higher than of the HOx source from ozone photolysis [*Possanzini et al.*, 2002]. *An et al.* [2009] reported that the photolysis of HONO, HCHO and O_3 contributed around 68, 25 and 7% of HOx, respectively, on a cloudless day in Beijing.

[7] Accurate formaldehyde measurements are crucial for understanding the atmospheric photochemistry of HCHO and its role in oxidation processes. Several techniques for determining atmospheric HCHO with a range of time resolutions and detection limits have been used over the last two decades. In particular, various spectroscopic techniques have been employed, including Fourier transform infrared spectroscopy (FTIR), differential optical absorption spectroscopy (DOAS), tunable diode laser absorption spectroscopy (TDLAS), and laser induced fluorescence (LIF) [*Lawson et al.*, 1990; *Harder et al.*, 1997; *Fried et al.*, 2003; *Wert et al.*, 2003; *Li et al.*, 2004; *Schwab et al.*, 2004; *Dasgupta et al.*, 2005; *Hottle et al.*, 2009]. Several continuous, automated solution phase methods have also been employed, such as the coil enzyme (CENZ) fluorometric method, dinitrophenylhydrazine (DNPH) derivatization techniques employing cartridges, coil/2, 4-dinitrophenylhydrazine (CDNPH), Hantzsch, diffusion scrubber/liquid fluorescence (DS/LF) and the cyclohexanedione diffusion scrubber (CHDDS) method [*Dong and Dasgupta*, 1987; *Lazrus et al.*, 1988; *Fan and Dasgupta*, 1994; *Zhou et al.*, 1996; *Lee et al.*, 1998; *Zhou et al.*, 2007]. Comparisons among different techniques for HCHO measurements have been the subject of many studies [*Lawson et al.*, 1990; *Heikes et al.*, 1996; *Gilpin et al.*, 1997; *Apel et al.*, 1998; *Cárdenas et al.*, 2000; *Fried et al.*, 2002; *Schwab et al.*, 2004; *Hak et al.*, 2005; *Apel et al.*, 2008; *Wisthaler et al.*, 2008]. In summary, during past intercomparison campaigns, the mean values obtained by various spectroscopic techniques, including the CENZ, CHDD, CDNPH, DS/LF, DNPH and Hantzsch methods are in reasonable agreement, but there is a general consensus that spectroscopic methods, especially those based on absorption are the most accurate, since they only depend upon carefully determined spectroscopic parameters.

[8] TDLAS is one of the most sensitive and selective direct methods for detecting small molecules in the atmosphere and is suited for HCHO determination [*Fried et al.*, 2002; *Wert et al.*, 2003; *Herndon et al.*, 2005]. It in particular has also been used in very-low HCHO level measurements [*Mackay et al.*, 1996; *Fischer et al.*, 1998; *Li et al.*, 2004]. Recent advances in infrared laser technology have led to the development of quantum cascade (QC) lasers, which have several advantages over lead-salt IR diode lasers including ease of operation and simpler deployment for field measurements [*Nelson et al.*, 2002]. These QC lasers can operate without cryogenic cooling at near-room temperature. With proper attention to laser mode purity and laser line width, this instrument does not require calibration, eliminating the demand for calibration mixture gases in the field [*Herndon et al.*, 2007].

[9] In the current work, HCHO in NYC was measured using a QC laser operating in the 5.67 μm wavelength region to determine HCHO in NYC during 2009 summer season. Here, we present the results from this study and discuss below (1) the characterization of HCHO in NYC, (2) partitioning of primary and secondary HCHO, (3) estimates of the major pathways for production of secondary HCHO within the polluted boundary layer, and (4) the contribution of HCHO to HOx radicals at this urban site.

2. Experiment

2.1. Sampling Site and Mobile Laboratory

[10] The field campaign was conducted from 15 July to 3 August 2009 on the campus of Queens College (40.73°N, 73.82°E, 25 m above sea level) in the borough of Queens, NYC. The neighboring area of this site is characterized by residential quarters. In addition to normal urban street traffic, there is a very busy 6- to 8-lane interstate, I-495 (Long Island Expressway, LIE), that runs east and west 0.6 km north of the site, and there are four additional 4- to 6- lane highways within a radius of 5 km.

[11] The SUNY Atmospheric Sciences Research Center Mobile Laboratory (ASRC-ML) was deployed for this summer campaign [*Schwab et al.*, 2010]. During most of the sampling period, the ASRC-ML was parked in parking lot 6 at the campus of Queens College, except for two mornings on 28 and 30 July, and two evenings on 27 July and 1 August when it was moved to parking lot 15 for the roadside measurements. There are two sample inlets, one for aerosol instruments and another for gaseous pollutants. Both gas and aerosol inlets are 2.5-cm O.D. stainless steel (SS) tubes mounted above the front roof on the driver's side. The sample flow was drawn into the mobile lab by a vacuum pump (Vacuubrand MD4) at a total flow rate of 63 lpm. The main aerosol sample flow (~17 lpm) for

Table 1. Instrumentation on the ASRC-ML Used at Queens During the 2009 Summer Campaign

Instrumentation	Measures	Time Resolution	LODs	Precision	Accuracy
Quantum Cascade Laser trace gas detector (ARI-QCL-76D)	HCHO	1 s	0.3 ppb	0.3 ppb	±6%
	NO_2	1 s	0.1 ppb	0.2 ppb	±3%
Ozone Monitor (2B Technologies Inc.- 202)	O_3	1 min	2 ppb	1.5 ppb	±2%
Nitric Oxide Monitor (2B Technologies Inc. −410)	NO	1 min	2 ppb	1.5 ppb	±2%
Nitrogen Oxides Monitor + NO2 converter(2B Technologies Inc. −401)	NOx	1 min	4 ppb	1.5 ppb	±2%
Aerosol Mass Spectrum (ARI)	Nitrate	5 min	4 ng/m^3		±20%
	Sulfate		5 ng/m^3		
	Ammonium		23 ng/m^3		
	Chloride		5 ng/m^3		
	Organics		57 ng/m^3		
Water-based Condensation Particle Counter (TSI-3781)	Aerosol number Conc.	1 s	1/cm^3		±10%
Fast Mobility Particulate Sizer (TSI-3091)	Particle Size	1 s			±10%
Photoacoustic Soot Spectrometer (DMT PASS)	Absorption Coefficient	1 s	0.2 1/Mm		±10%

aerosol devices was drawn into the mobile lab through a 2.5-cm O.D. SS tube that protruded 37 cm through the front roof. This flow-passed through the in-line cyclone to remove larger particles (>2.5 μm). The gas flow made up the remainder of the 63 lpm (~46 lpm) and was drawn into the van through a 1.9- cm O.D. PFA Teflon tube inserted into the second SS manifold tube extending 37 cm forward of the front roof. Once inside the vehicle the flow was split between the sampling instruments and the remaining flow was exhausted through the pump as bypass flow. The QCL instrument drew ~4 lpm of flow into the multipass absorption cell through a ~1.5 m of 1.9-cm O.D. PFA Teflon tube followed by ~2 m of 9.4-cm O.D. PFA Teflon tube.

2.2. Instrumentation

2.2.1. QCL Trace Gas Detector

[12] Ambient HCHO concentrations were determined by a dual quantum cascade laser trace gas detector (QCL, Model QCL-76-D), fabricated by Aerodyne Research, Inc. (ARI). The QCL system has been described in detail by *Herndon et al.* [2007] and only a brief description will be given here. The QCL trace gas detector consists of two main modules: an optical bench and an electronics module. The optical apparatus is constructed on a 63 cm by 43 cm aluminum honeycomb table which contains one liquid-nitrogen-cooled Dewar for temperature control of detectors, optics for laser beam collection and transport, and an astigmatic multipass absorption cell. The electronics module contains a computer-controlled system that incorporates the electronics for driving the two QC lasers (in our case one for HCHO and another for NO_2) along with signal generation and signal acquisition. The optical table is enclosed by a rigid aluminum cover when in use and is thermally stabilized (temperature was controlled at 30 ± 0.5°C) by heating elements attached to the base of the optical table and to the aluminum cover. The optics collects the light from two pulsed lasers (operating in non-overlapping time windows) into a pair of beams that are directed into an astigmatic multiple pass absorption cell (path length = 76 m, volume = 0.5 l for atmospheric sampling at a pressure of 58–60 Torr) and then imaged onto a single liquid nitrogen cooled HgCdTe photovoltaic detector. In addition to the main optical beam, a portion of each laser beam is sent to a reference cell containing a high concentration of the gas of interest (in this study, the reference cell was filled with HCHO). We used the commercial distributed feedback (DFB) InGaAs-AlInAs/InP QC lasers (Alpes Laser, Switzerland) designed for pulsed operation at near room temperature. Selection of the molecular absorption feature for a given laser is achieved by temperature tuning, from −40 ~ 40°C using a two-stage Peltier element. The laser wavelength is swept, using a current ramp and temperature modulation, over a narrow region (<1 cm^{-1}) at a repetition rate around 2.5–7.0 kHz with synchronous detection of the transmitted light. The data software "TDLWINTEL" developed by ARI sweeps the laser frequency over the full infrared transitions or group of transitions, then integrates the area under the transitions by using a low-order polynomial fit to the known spectral line shapes and positions. However, the species concentrations are tied to the absolute spectroscopic data found in the HITRAN database [*Rothman et al.*, 1998]. Given that the line strengths in the database are absolute numbers, the instrument does not require calibration, eliminating the need for calibration gas in the field.

[13] An ideal wavelength region for detection of HCHO is in the ν_2 band at 1764.902 cm^{-1}. The peak absorbance depth for simulation HCHO is ~5.2×10^{-5} for 1 ppb (a laser line width of 0.01 cm^{-1}, 60 Torr). One strong water line is at 1764.694 cm^{-1}, and a relative weak H_2O line is at 1764.858 cm^{-1}. In the fitting procedure, two H_2O absorption features were fit as the second and third species to eliminate them as interference to the HCHO measurements. The limit of detection (LOD) for HCHO measured by QCL trace gas detector is 0.3 ppb (see in Table 1). Before and after this campaign, we checked the linearity and precision of this fitting procedure. A 3.95 ppm HCHO standard gas purchased from Scott Inc. was diluted to 1.6, 2.4, 3.2, 4.0, 7.9, 11.9, 15.8, 23.7, 31.6, and 39.5 ppb using a second cylinder of zero air as the diluent. The results showed a linear "calibration curve" with a slope and coefficient of determination (R^2) equal to 1.06 and 0.999, respectively. This confirmed the HCHO line strengths used for QCL measurements.

2.2.2. Other Instruments

[14] Table 1 lists all the instruments deployed in ASRC-ML during the summer campaign. NO and NOx were measured every 60 s from the detection of ozone depletion by UV absorption at 254 nm (2B Technologies Inc., models 400 and 410) with a rated precision of 1.5 ppb below 65 ppb concentration. O_3 mixing ratios were observed from UV absorption measurements (2B Technologies Inc., model 202)

which have the same rated precision specification. For aerosols, an ARI High-Resolution Time-of-Flight Aerosol Mass Spectrometer (HR-ToF-AMS) was used to measure the composition and size distributions of inorganic and organic aerosols at 1–5 min time resolution [*Sun et al.*, 2011]. A water-based condensation particle counter (WPCP, TSI 3781) provided 1-min data of aerosol number concentrations with a rated lower diameter cutoff of 6 nm. A fast mobility particulate sizer (FMPS, TSI 3091) and photoacoustic soot spectrometer (DMT PASS1) with time resolution of 1 s were employed to determine particle size distribution in the range of 5.6 to 6000 nm and absorption coefficient of black carbon (BC), respectively. The BC mass concentrations were determined from the PASS results using a calibration factor verified in laboratory calibrations. In addition to measurements from the mobile facility, hourly methane (CH_4), non-methane organic carbon (NMOC) concentrations and meteorological parameters (including relative humidity, wind speed and wind direction) were also observed in NYSDEC (New York State Department of Environmental Conservation) Air Monitoring Building located ~140 m north of parking lot 6. Moreover, a daily 24-h integrated VOC canister was collected outside the building during the experimental period. These experiments are parts of the Photochemical Assessment Monitoring Station (PAMS) program conducted by NYSDEC. CH_4 and NMOC were measured by using a commercial CH_4/NMOC analyzer (Horiba APHA 360). This instrument uses selective combustion and flame ionization detector (FID) for determining CH_4 and NMOC in the air. However, the standard approach for daily VOC analysis was based upon gas chromatography (GC) combined with mass spectrometry (MS). The details were discussed by *Parrish and Fehsenfeld* [2000]. This technique offers increased sensitivity for determining VOC species. On average, the LODs for most VOC species determined by GC-MS were in the range of 0.1–0.5 ppb and the accuracy was within ±15%.

3. Results

3.1. Typical HCHO Patterns

[15] The summer campaign was conducted from 15 July to 3 August at the Queens Campus. At the start of the period, the comparatively strong high pressure system moved through NYC, resulting in the clear skies and narrow ranges of both high (28 ± 2°C) and low temperature (18 ± 2°C) variations. Starting 21 July, a series of weak front of all sorts (warm, cold, stationary etc.) passed over this city. This caused low air temperature and strong precipitation occurred on some of the rest days. On the other hand, the diurnal variation of wind field was significant (see Figure 2). Except for traffic rush hours, the prevailing wind at this site was from the southwest and the wind speed was usually less than 2 m/s. Figure 1 shows the time series plot of HCHO, NO, NO_2, NOx, O_x (=NO_2 + O_3), BC, total SOA (=semivolatile OOA + low volatility OOA + nitrogen-enriched organic aerosol factor [*Sun et al.*, 2011]) and meteorological parameters in NYC. Ambient HCHO concentrations were measured from 16 July to 3 August 2009. The mixing ratios of formaldehyde ranged from 0.4 to 7.5 ppb with a mean value of 2.2 ± 1.1 ppb (The median value of HCHO was 2.0 ppb). This value was in line with those observed in downtown Denver (2.7 ppb), and Philadelphia (3.1 ppb) [*Anderson et al.*, 1996; *Dasgupta et al.*, 2005], but was lower than that measured in midtown Atlanta (8.8 ppb) by a factor of 3.6 (see Table 2). This high HCHO level in Atlanta was attributed to diesel engine exhaust from a bus repair depot [*Dasgupta et al.*, 2005]. In Houston, *Dasgupta et al.* [2005] showed that a maximum HCHO concentration reached 47 ppb, probably produced from the oxidations of HCHO precursors such as ethene and propene. However, the summertime HCHO concentrations at the rural sites ranged from 0.8 to 1.4 ppb, consistently lower than those in urban areas.

[16] Figure 2a illustrates the diurnal variations of HCHO, Ox, O_3, NO, NOx, total SOA and BC concentrations at Queens during the field measurement. The diurnal patterns of wind speeds and wind directions are also shown in Figure 2a. HCHO exhibited strong diurnal variations during the field measurements as shown in Figure 2a. HCHO concentrations typically reached the peak by 1100 (Eastern Standard Time, EST) to midday, decreased gradually in the afternoon, and remained low at night. O_3 rose to its maximum at 1300 EST - 1400 EST which was one to two hours later than the HCHO peak. This might reflect the fact that HCHO is one of the precursors of ozone. In addition, the diurnal profile of the concentrations of total oxygenated organic aerosol (OOA-a surrogated for secondary organic aerosols [*Zhang et al.*, 2007]) determined by the HR-ToF-AMS also peaked between 1200 EST–1300 EST [*Sun et al.*, 2011]. The traffic-related species such as NO, NOx and BC levels remained constant throughout the early morning until about 0500 EST, reached the maximum at 0600 EST, and then decreased through the late morning and afternoon. The high NO, NOx and BC levels between 0500 EST and 0800 EST could be attributed to the fresh emissions from busy traffic into the still low boundary layer. On the other hand, the wind direction might influence the diurnal patterns of these primary pollutants during the sampling period. The winds during 0400 EST–0800 EST were observed to be mainly from the northwest, directly impacted by the LIE. Thus, the high NO, NOx and BC might be also associated with the traffic emissions from LIE. The declining trends of these primary pollutants during late morning and afternoon hours are due to the growth of the boundary layer combined with photochemical transformation and deposition processes.

[17] Correlation analysis between HCHO and NOx, BC and Ox can provide the information of potential source of HCHO. In this study, the correlation analysis was made by using the hourly data of each air pollutant. Figure 2b illustrates the R values of HCHO with NOx, BC and Ox. During the morning rush hours, HCHO correlated strongly with BC and NOx ($R > 0.6$, being required for its significance), suggesting that a significant contribution to HCHO came from primary sources (since NOx and BC are the primary pollutants emitted by vehicle emissions). In contrast, a good correlation between HCHO and O_x ($[O_x] = [NO_2] + [O_3]$) was observed near noontime. Good correlation between HCHO and O_x, and the occurrence of strong solar radiation and high ambient temperature strongly suggests that the HCHO peak at noontime was mainly due to photochemical reactions.

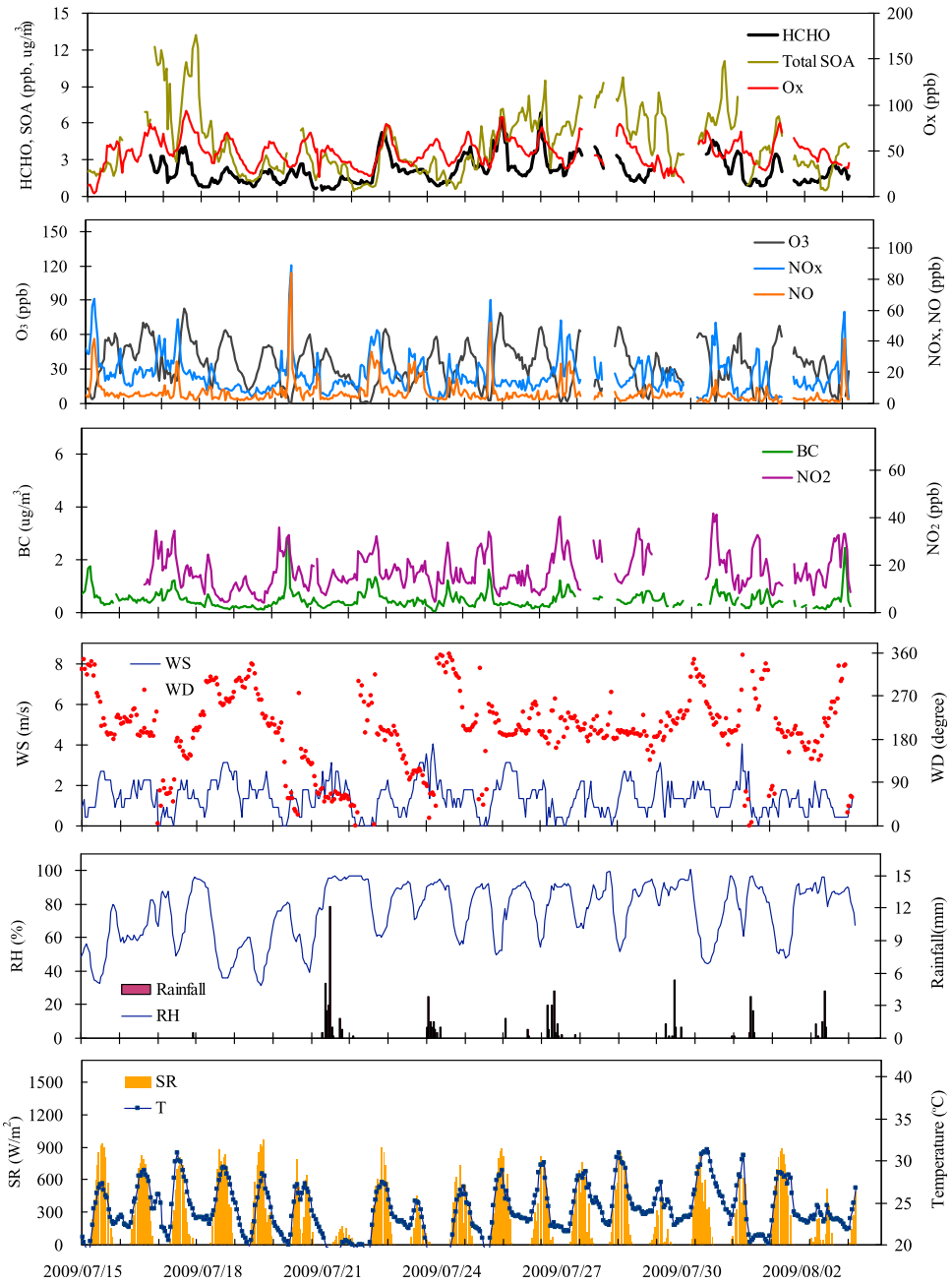

Figure 1. Time series of HCHO, total SOA, Ox (O_3 + NO_2), O_3, NOx, NO, NO_2, particulate BC, and meteorological parameters observed at Queens College during the sampling period.

3.2. Partitioning of Primary and Secondary HCHO

[18] To understand how much daytime formaldehyde was formed by photochemistry, we examine the ratios of HCHO/NOx and HCHO/BC [*Lawson et al.*, 1990]. Figure 3a shows the diurnal variations of HCHO/NOx and HCHO/BC ratios at the Queens site. In Figure 3a, the solid diamonds and circles represent the hourly means of HCHO/NOx and HCHO/BC at the Queens, respectively. The bars denote the standard deviations. The diurnal patterns of HCHO/NOx were similar to those of HCHO/BC. The ratios remained relatively flat between 2300 EST and 0400 EST throughout the study period. During the sampling interval from 0500 EST to 0800 EST (morning traffic peak) when NOx and BC increased rapidly, both ratios decreased. From 0900 EST, the ratios increased substantially and remained at high values until late afternoon hours. In NYC, both BC and NOx are emitted from traffic sources [*Venkatachari et al.*, 2006]. BC is more "stable" than NOx as it does not strongly participate in photochemistry. Thus, we use the HCHO/BC ratios to partition primary and secondary HCHO. The photochemical HCHO percentage was estimated using the differences of this ratio between ambient ($[HCHO/BC]_a$)

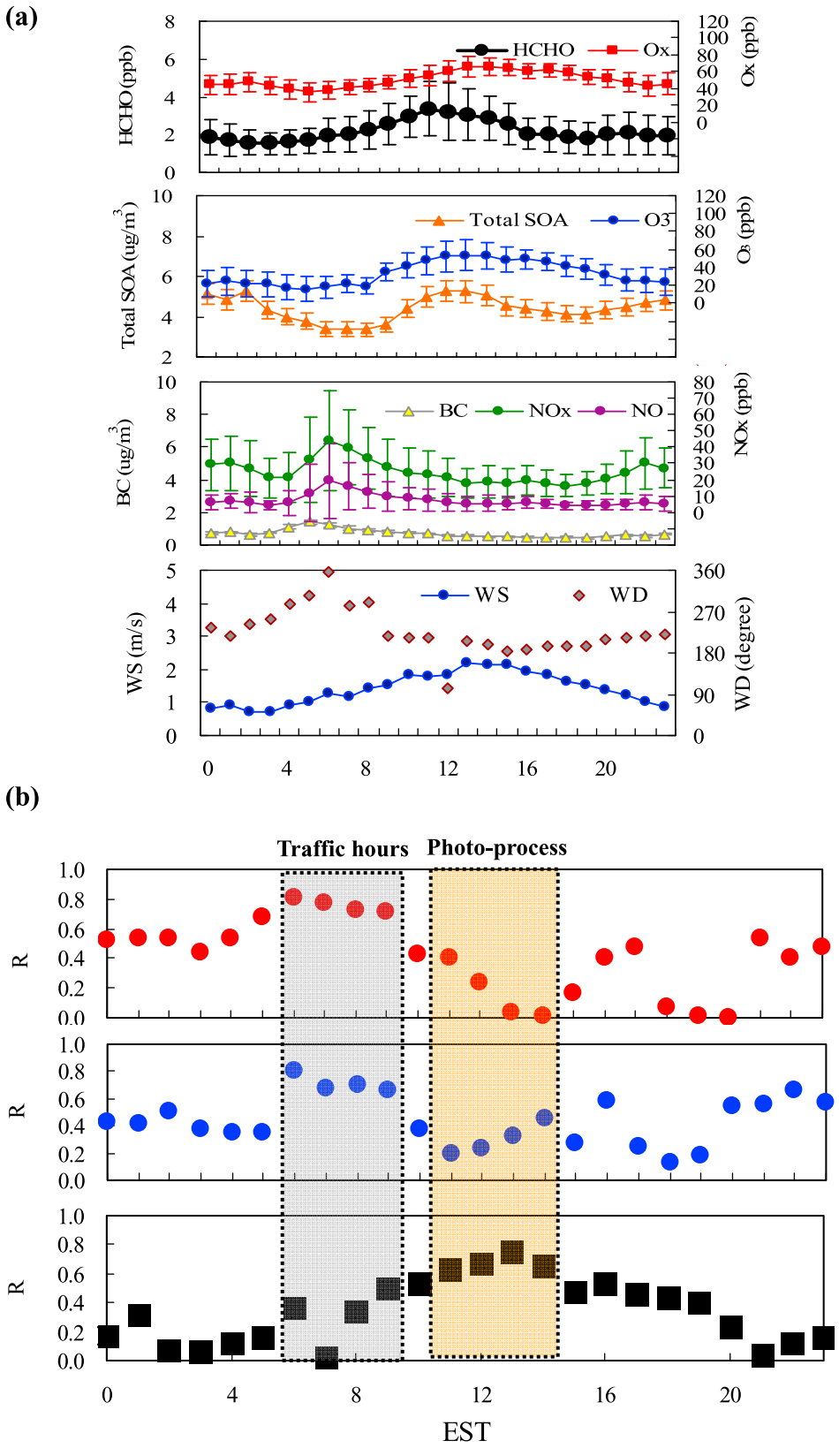

Figure 2. Diurnal patterns of (a) air pollutant concentrations, wind speed and wind direction, and (b) correlation coefficients between HCHO and other air pollutants in NYC.

Table 2. Comparisons of Summertime HCHO Concentrations (ppb) Observed at Various Urban and Non-urban Sites

Sampling Sites	Mean	Max	Min	Reference[a]
Urban Areas				
New York City, NY, USA	2.2	7.5	0.2	This work
Nashville, TN, USA	5.1	12.7	1.4	1
Atlanta, GA, USA (near a bus repair depot)	8.0	18.3	0.4	1
Houston, TX, USA (heavy industrial region)	4.5	47.1	0.2	1
Philadelphia, PA, USA	3.1	9.5	0.3	1
Denver, CO, USA	2.7			2
Houston, TX, USA (parking lot)	5.6	24.0		3
Mexico City, Mexico (parking lot)	4.3	20.1		4
Milan, Italy	3.6	8.0	0.4	5
Takasaki, Japan	4.3	11.4	2.5	6
Rural Area				
Whiteface Mountain, NY	1.4	4.7	<0.1	7
Mazhuang, east China	1.5	6.2	0.2	8
Schauinsland, Germany	1.5	2.8	0.2	9
Quebec, Canada	0.8	4.8	<0.1	10

[a]References: 1, *Dasgupta et al.* [2005]; 2, *Anderson et al.* [1996]; 3, *Chen et al.* [2004]; 4, *Grutter et al.* [2005]; 5, *Hak et al.* [2005]; 6, *Satsumabayashi et al.* [1995]; 7, *Li et al.* [2004]; 8, *Wang et al.* [2010]; 9, *Slemr et al.* [1996]; 10, *Macdonald et al.* [2001].

and fresh emission plume ($[HCHO/BC]_{pri}$) by the following equation:

$$f^{sec}_{HCHO} = \left([HCHO/BC]_a - [HCHO/BC]_{pri}\right)/[HCHO/BC]_a \quad (1)$$

where f^{sec}_{HCHO} is the fraction of secondary HCHO. In this equation, the emission ratio of HCHO/BC for fresh emission plumes ($[HCHO/BC]_{pri}$) was estimated by using roadside measurement results near the LIE during this campaign. Figure 3b shows the scatterplot and least squares linear regression of 1 - min average HCHO and BC concentrations conducted on 28 July (0600–0700 EST) and 1 August (1800–1900 EST) near the LIE [*Sun et al.*, 2012]. During the roadside measurements on July 28 morning and August 1 evening, the traffic flow rate of LIE was 9600 vehicles/hr, and approximately 12% were diesel truck vehicles. The good correlation between HCHO and BC ($r^2 = 0.87$) suggested a strong association between HCHO and traffic emissions. The slope and intercept for the simple linear regression were 2.82 ± 0.11 and 0.99 ± 0.07, respectively. The nonzero intercept reflects the local and regional background concentrations of HCHO from accumulated direct emissions and photochemically produced HCHO. Indeed, the intercept of 0.99 ppb was consistent with the average HCHO concentration (1.4 ppb) observed at Whiteface Mountain, NY (Table 2), where fresh primary emissions are limited. The slope of 2.82 can be taken to represent the fresh ratio of HCHO/BC from the primary emissions at this location, and the statistical uncertainty for this ratio was approximately 4%. The slope determined from Figure 3b - 2.82 ppb-HCHO/ug/m^3-BC - is taken to be the emission ratio (ER) of HCHO/BC from the LIE (mixed vehicle condition). Using the ER value we could roughly estimate that the BC/CO from LIE was approximately 1.1 μg/m^3-BC/ppm-CO since measured ratios for HCHO to CO of approximately 3 ppb-HCHO/ppm-CO have been observed from "chase" experiments [*Herndon et al.*, 2005] and tail pipe emissions [*Schauer et al.*, 2002] conducted in U.S. domestic regions. This inferred BC/CO ratio of 1.1 is in reasonable agreement with the value of 1.6 observed in Mexico City [*Jiang et al.*, 2005]. We then use this ER to estimate the secondary HCHO by using equation (1). Figure 3c reveals the estimates of diurnal distributions of primary and secondary HCHO in NYC. The primary HCHO (including background HCHO) dominated over this region from 0000 EST to 0800 EST, with a significant enhancement during busiest traffic periods. After 0900 EST, the contributions of secondary sources to ambient HCHO exceeded the primary emissions and reached a maximum between 1200 EST and 1500 EST (>70%), then decreased gradually and remained at 50–60% after sunset. On average, daily secondary HCHO was estimated to be approximately 70% of the total ambient HCHO. Previous studies employed different techniques to separate primary and secondary HCHO in urban areas. For example, *Harley and Cass* [1994] estimated the primary and secondary HCHO in several urban cities of southern California by using an Eulerian photochemical air quality model. They found that photochemical production contributed a large of ambient HCHO during daytime while mobile source emissions were a major contributor to HCHO during busy traffic hours. *Possanzini et al.* [2002] used the ratio of HCHO/toluene in fresh emissions and ambient air in Rome, Italy, and suggested that secondary production increased strongly in summertime where it reached as high as 80% in the warmest hour of the day. In Mexico City, *Garcia et al.* [2006] partitioned primary and secondary HCHO according to the linear regression of HCHO-CO-CHOCHO, and they found that secondary HCHO accounted for ~40% of the ambient HCHO. *Rappenglück et al.* [2010] suggested primary vehicle emissions, secondary photochemically and industrial emitted HCHO accounted approximately 39%, 24% and 9% respectively, to the total measured HCHO in Houston during the summertime 2006. The remaining 28% of HCHO (the residual) could not be associated with the above sources, but might be attributed to the HCHO transported to the sampling site. The primary HCHO source was mainly from vehicle and industrial emissions [*Buzcu Guven and Olaguer*, 2011], while secondary HCHO was attributed to the oxidation of isoprene, methane, PAN and alkenes [*Lee et al.*, 1998].

3.3. Photochemical Production of Formaldehyde

[19] To provide an assessment of the relative secondary HCHO production expected from oxidation of VOCs, we calculate the "HCHO production rate" (F_p) from individual VOC using the daily canister VOC measurement results. The F_p value can be estimated from [*Lee et al.*, 1998]:

$$F_p = \sum\left(k_{iOH} \times [VOC]_i \times \gamma_{HCHO\,(VOCi)} \times [OH]\right) \quad (2)$$

where k_{iOH} is the reaction rate constant between VOC species i and OH radicals. The daily average concentrations of VOC species and the k_{iOH} reaction rate constant between VOC and OH are listed in Table 3. As can be seen in Table 3, the k_{iOH} of alkenes are generally one order higher

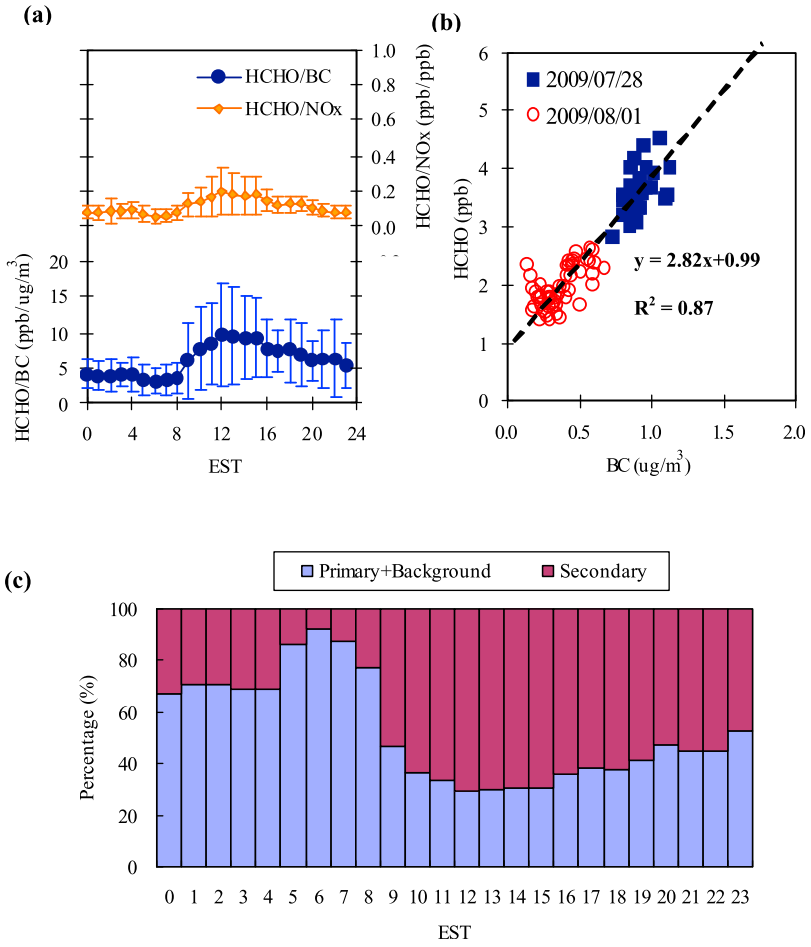

Figure 3. Diurnal variations of (a) ratios for HCHO/NOx and HCHO/BC, and (c) partitioned primary and secondary HCHO concentrations. Orange and blue dots represent the ratios for HCHO/NOx and HCHO/BC. (b) The scatterplot between HCHO and BC measured near LIE on 28 July (0600–0700 EST) and 1 August (1800–1900 EST) during this campaign is also plotted.

than those of alkanes. Isoprene has the fastest k_{iOH} among the listed species (11×10^{-11} cm^3/molecules/s), whereas methane has the slowest (6.4×10^{-15} cm^3/molecules/s). $[VOC]_i$ is the concentration of VOC species i, and $\gamma_{HCHO\ (VOCi)}$ is the HCHO yield of each VOC species (see Table 3). The HCHO yields for isoprene and propene were 0.66 and 1.0, respectively [*Lee et al.*, 1998; *Sprengnether et al.*, 2002]. The HCHO yields for methane and isobutane were assumed to be 1.0 and 0.8, and those of other alkanes ranging from 0.1 to 0.3 were used [*Lee et al.*, 1998]. For alkenes, HCHO yields ranging from 0.0 to 1.0 were assumed, while those for aromatic compounds $\gamma_{HCHO\ (VOCi)}$ were set to be zero (see Table 3). [OH] is the concentration of hydroxyl radicals. OH concentrations were not measured during this field campaign, and therefore we used the OH values from *Ren et al.* [2003a]. They determined the 1- min OH mixing ratios by using a laser-induced fluorescence instrument at Queens College during the $PM_{2.5}$ Technology Assessment and Characterization Study-New York (PMTACS-NY) intensive in summer 2001. During PMTACS-NY2001, the daily average OH concentration was 2.4×10^6 molecules/cm^3. We thus used the OH value combined with daily canister VOC data to assess the F_p by using the equation (2). Figure 4 shows the daily average contributions of isoprene, methane, alkanes and alkenes to HCHO photochemical production in NYC during this campaign. Using the OH values of $\sim 2.4 \times 10^6$ molecules/cm^3, the daily average F_p was determined at approximately 0.44 ppb/hr. On average, 44% of the formaldehyde production was associated with isoprene oxidation by the OH radicals. Methane and propene contributed, respectively, 25 and 18% to the HCHO formation. The other alkanes and alkenes accounted for less than 7% of the HCHO formation. This suggests that the secondary HCHO in NYC was mainly produced from the oxidation of isoprene, methane and propene during this study. We also estimated the diurnal variations of secondary HCHO production from isoprene, methane and propene which required hourly data for isoprene, methane and propene. Since except for methane, hourly concentrations of propene and isoprene were not measured at Queens College during the sampling period, we used the 24-h canister data from the Queens site, along with canister and hourly data from a station in the neighboring borough of Bronx to estimate the diurnal pattern of isoprene and propene at the Queens site. The sampling station in Bronx was at the New York Botanical Gardens, which is located approximately

Table 3. Overview of the VOCs Used to Derive HCHO and HOx Productions in This Study

Species	Average Conc.[a] (ppb)	$k_{iOH} \times 10^{-11}$ [b] (cm^3/#/s)	HCHO Yields	$k_{iO3} \times 10^{-18}$ (cm^3/#/s)	OH Yield
		Alkanes			
Methane	2043	0.00064	1.00		
Propane	1.27	0.11	0.15		
n-Butane	0.53	0.24	0.40		
iso-Butane	0.37	0.22	0.80		
Pentane	0.32	0.40	0.30		
2,2-Dimethylbutane	0.02	0.23	0.00		
iso-Pantane	0.70	0.37	0.50		
2-Methylpentane	0.14	0.53	0.35		
3-Methylpantane	0.11	0.54	0.35		
n-Hexane	0.15	0.53	0.30		
n-Heptane	0.06	0.70	0.30		
Methylcyclohexane	0.03	1.00	0.00		
Octane	0.02	0.87	0.30		
Nonane	0.04	1.00	0.30		
Decane	0.06	1.12	0.30		
		Alkenes and Aromatics			
Propene	0.31	3.00	1.00	10.1	0.35
trans-2-Butene	0.01	6.40	0.00	190.0	0.64
cis-2-Butene	0.02	5.64	0.00	125.0	0.37
1-Pentene	0.03	3.14	1.00	10.0	0.24
cis-Pentene	0.03	6.70		140.0	0.30
trans-Pentene	0.02	6.50		160.0	0.47
Isoprene	0.31	11.00	0.66	12.80	0.13
1,3-Butadiene	0.03	6.76	0.58	6.30	0.13
Benzene	0.17	0.12	0.00		
Toluene	0.47	0.60	0.07		
Ethylbenzene	0.05	0.71	0.00		
m/p-Xylene	0.18	1.90	0.00		
o-Xylene	0.06	1.37	0.00		
iso-Propylbenzene	0.01	0.65	0.00		
n-Propylbenzene	0.01	0.60	0.00		
1,3,5-Trimethylbenzene	0.02	5.75	0.00		
1,2,3-Trimethylbenzene	0.02	3.25	0.00		
1,2,4-Trimethylbenzene	0.06	3.25	0.00		

[a]The VOC concentration was obtained form the average value of 18 daily VOC canister data observed in NYSDEC Air Monitoring Building. All the VOC canisters were 24-h samples.
[b]All the reaction rate constants listed in this table in the condition of 298 K.

7 km to the northwest. It is maintained by the New York State Department of Environmental Conservation (NYSDEC). The hourly VOC observation at Bronx is also a part of PAMS program. The method for atmospheric hydrocarbon measurements is based on GC separation of the individual hydrocarbons and the detection of each using a flame ionization detector (FID). The detail of this automated GC method was discussed by *Oliver et al.* [1996]. On average, the LODs for most of VOCs can be under 0.5 ppb. However, ethylene, i-butene and 1-butene were not included in the VOC measurements during the PAMS program. For isoprene, we assumed that the diurnal variation profile at Queens College is as the same as that in Bronx. Consequently, the hourly variability of isoprene at Queens College ($[isoprene]_{QC\text{-}i}$) can be estimated from

$$[isoprene]_{QC-i} = [isoprene]_{QC-daily} \times \left(\frac{[isoprene]_i}{[isoprene]_{daily}} \right)_{Bronx} \quad (3)$$

where $[isoprene]_{QC\text{-}daily}$ are the 24 h average isoprene concentrations at Queens College; $([isoprene]_i/[isoprene]_{daily})_{Bronx}$ is the ratio of hourly isoprene concentration to the 24 h daily mean in Bronx. A further complication arises because hourly propene concentrations were not available due to an interference in the hourly GC method. For estimating the diurnal profile of propene, we first find the ratio (C = [propene]/

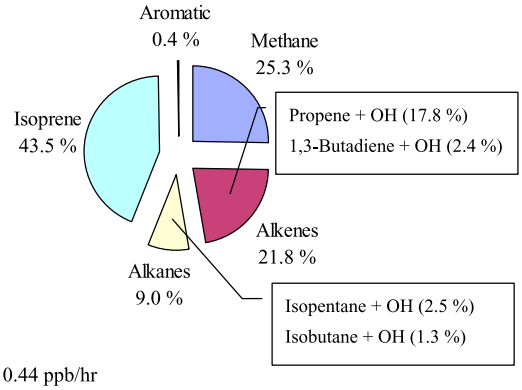

Figure 4. Relative contributions of isoprene, methane, alkenes and alkanes to HCHO production, estimated using [OH] = 2.4×10^6 molecules/cm^3. The data represents diurnal variability since the contributions may differ during the day.

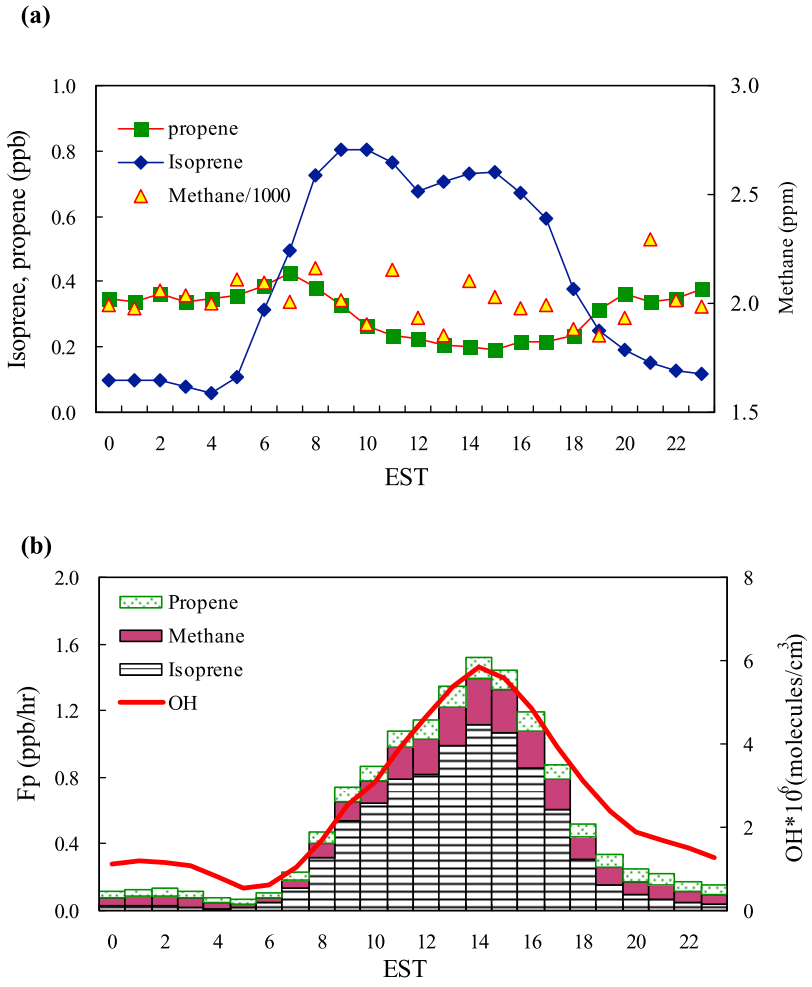

Figure 5. Diurnal patterns of (a) the mixing ratios for propene, methane and isoprene and (b) Fp contributed from propene, methane and isoprene at Queens College during the campaign. In Figure 5a, the diurnal profiles of isoprene and propene were obtained by calculation which is described in the text. The OH concentrations shown in Figure 5b are based on the data measured by *Ren et al.* [2003a].

[isopentane]) of daily averaged propene to daily average isopentane at Queens College. The reasons for selecting isopentane include (1) propene and isopentane are mainly from common sources, such as motor vehicles [*Seinfeld and Pandis*, 1998]; (2) the daily isopentane concentrations measured at Queens College and in Bronx correlated well with the slope close to unity; and (3) the ambient concentrations of isopentane were high enough to give us good signal-to-noise and consequently lower uncertainty. Next, we assumed that the C value is consistent at both Queens and Bronx sampling sites. Based on these assumptions, the estimated diurnal profile of propene at the Queens site ($[propene]_{QC\text{-}i}$) was then obtained as

$$[propene]_{QC-i} = [isopentane]_{Bronx-i} \times C \qquad (4)$$

where $[isopentane]_{Bronx\text{-}i}$ is the hourly concentration at Bronx. To check this result we also selected other species such as n-butane, n-hexane and toluene for the estimations. Similar diurnal patterns of propene were obtained by using the four different species in the calculations. Figure 5a shows the average diurnal profiles of propene, isoprene and methane at Queens College. In NYC, higher isoprene concentrations were observed during the daytime. For propene, the significant diurnal cycles were found with higher concentrations during the traffic hours. The lower levels during daytime were explained by its sink due to oxidation by OH radicals and O_3. In Figure 5b, we present the results of average diurnal patterns of HCHO production by isoprene, methane and propene. The average diurnal cycles of OH are also plotted in Figure 5b. The hourly OH mixing ratio shown here were calculated from the 1-min OH data which measured by *Ren et al.* [2003a] in the PMTACS-NY campaign in summer 2001. Secondary HCHO production rate from VOC precursors was roughly constant (0.12 ppb/hr) before sunrise. During this low Fp period, methane and propene were the major precursors for HCHO since the isoprene concentrations was lower than 0.1 ppb. After 0500 EST the Fp increased drastically, reaching to the maximum values at 1400 EST (1.5 ppb/hr). The significantly elevated Fp during daytime was associated with the increased OH and isoprene concentrations. Quite clearly, isoprene is the major source of secondary HCHO during this period. After sunset, the OH concentrations decreased again, resulting in lower HCHO

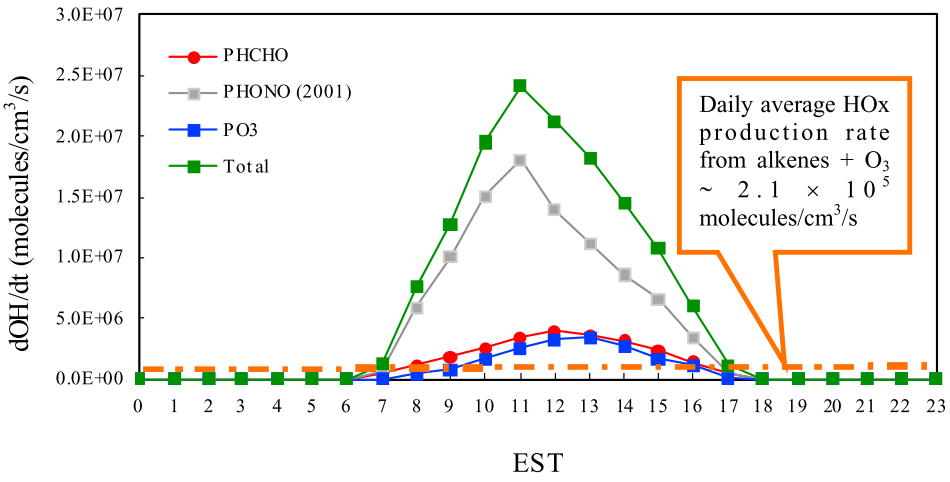

Figure 6. Diurnal variations of HOx production rates from photolysis HCHO, HONO and O_3 in New York City. The orange solid-dash line represents the daily average of HOx production rate from alkenes + O_3.

production rates; during this period HCHO was mainly produced by the reactions of methane and propene with OH radicals. Note that our study of HCHO yield only takes into account first generation products of OH-initiated VOC oxidations. Production of moderately long-lived species, such as acetaldehyde, was not considered. For example, peroxyacetyl nitrate (PAN) is another important precursor of HCHO formation in polluted atmospheres. The formation of HCHO from PAN is not as direct a pathway as the reactions of VOCs and OH radicals. The decomposition of PAN produces the peroxyacetyl radical ($CH_3(CO)O_2$), which can react with NO and RO_2 to form HCHO. *Lee et al.* [1998] found a rate of HCHO production from PAN decomposition of around 0.29 ppb/hr ([OH] was assumed to be 10^7 molecules/cm^3), accounting for 12% of the total HCHO generation during the 1995 Nashville/ Middle Tennessee Ozone Study. Some studies suggested that the oxygenated carbon compounds also contributed to ambient HCHO. For example, *Sumner et al.* [2001] suggested that the oxidation of Methacrolein (MACR) and Methyl Vinyl Ketone (MVK) contributed approximately 1.5% to ambient HCHO during the PROPHET summer campaign. *Macdonald et al.* [2001] suggested that the contribution of CH_3CHO to HCHO was approximately 3% in Quebec remote site. These oxygenated carbon compound may be a minor source of HCHO compared with isoprene, methane and propene. In this study, we did not have any data to show the contribution of oxygenated carbon compounds to HCHO in NYC. Consequently, the calculated production rate of HCHO in this study was underestimated since we did not include the oxidation of PAN and other oxygenated compounds in the calculations.

3.4. HOx Production

[20] HOx radicals are arguably the most important oxidants in the atmosphere. They participate in the production cycles of ozone, acidic gases and organic aerosol. In the polluted urban atmosphere, HOx production from HCHO (R3) can be as important as that from HONO photodecomposition (R8), or from O_3 photolysis followed by reaction of (O^1D) and water vapor as shown in reactions R5–R7. Apart from the photolysis of these oxygen-containing species, HOx production from the reaction of alkenes +O_3 can also contribute in urban areas [*Alicke et al.*, 2002; *Ren et al.*, 2003b]

$$O_3 + h\nu \rightarrow O(^1D) + O_2;\ \lambda \leq 320\,\text{nm} \quad \text{(R5)}$$

$$O(^1D) + M \rightarrow O(^3P) + M \quad \text{(R6)}$$

$$O(^1D) + H_2O \rightarrow 2OH \quad \text{(R7)}$$

$$HONO + h\nu \rightarrow OH + NO;\ 300\,\text{nm} \leq \lambda \leq 405\ \text{nm}. \quad \text{(R8)}$$

[21] In this study, we assessed the HOx production rate from measured data and tried to identify which species are important sources of ambient HOx. The total HOx production rates from the photolysis of HCHO, HONO and O_3 can be estimated as

$$(P_{HOx})_{photolysis} = 2j_{HCHO}[HCHO] + j_{HONO}[HONO] + 2j_{O3}\frac{k_7[H_2O][O_3]}{(k_6[M] + k_7[H_2O])} \quad (5)$$

where k_6 and k_7 are the reaction rate constants of reactions R6 and R7. M is the concentration of air. j_{HCHO}, j_{O3} *and* j_{HONO} are the photolysis rate constants of R3, R5 and R8, respectively. The photolysis rate constants were computed using online NCAR Tropospheric Ultraviolet and Visible (TUV) Radiation Model (http://cprm.acd.ucar.edu/Models/TUV/). The ozone column and surface albedo were set to be 289 du and 0.044, respectively. HONO concentrations were obtained from measurements at the Queens College site during PMTACS-NY2001 summer field campaign [*Zhou et al.*, 2004]. In the past decade, the decreasing trends of air pollutant levels in the cities of the world were due to reductions of mobile emissions [*Ban-Weiss et al.*, 2008; *von Schneidemesser et al.*, 2010]. In NYC, the declining rates of CO, NOx and O_3 were, respectively, −4% −3.2% and −2.0% per year between 2001 and 2010. This indicated that

OH and HONO concentrations in 2009 might be lower than those in 2001 of 20–40% as the trends of CO and NOx might suggest. Thus, the effect of such trends on our analysis would be on the order of 20–40%. However, the effect is only for the magnitude of Fp (section 3.3) and HOx production rate, but is not for the relative contributions.

[22] The HOx production rates from alkenes + ozone can be estimated as

$$(P_{HOx})_{alkenes+O3} = \sum\left(k_{iO3}\cdot[O_3]\cdot[Alkenes]_i\cdot\gamma_{iHOx}\right) \quad (6)$$

where k_{iO3} and γ_{iOH} are, respectively, the reaction rate constant between O_3 and alkenes i, and HOx yields as listed in Table 2. All the reaction rate constants of alkenes and ozone and HOx formation yields were taken from *Atkinson* [1997] and *Paulson et al.* [1999].

[23] Figure 6 shows the diurnal variations of the calculated HOx production rates from HCHO, HONO, and O_3. As can be seen in Figure 6, the daily HOx production rates averaged $\sim 1.3 \times 10^7$ molecules/cm^3/s, and the maximum value of 2.4×10^7 molecules/cm^3/s was observed at 1100 EST, coinciding with the HONO peak. The production rate of 1.3×10^7 molecules was comparable to those in Milan, Rome and Beijing [*Alicke et al.*, 2002; *Possanzini et al.*, 2002; *An et al.*, 2009]. As shown in Figure 6, HONO is the most important source of daytime HOx radicals in NYC, accounting for 67%, followed by HCHO (18%) and O_3 (13%). However, the alkene ozonolysis accounted for less than 2% to the total HOx production. In Santiago Chile, *Elshorbany et al.* [2009] employed both Mater Chemical Mechanism (MCM), and a simple quasi-photostationary-state model (PSS) with simultaneous measured data to evaluate the OH budget. The found that the HONO photolysis was also the most important primary OH source comprising ~55% to the OH production, followed by alkene ozonolysis (~24%), photolysis of HCHO (~16%), and O_3 (~5%) during daytime. On daily average, the contribution of alkenes $+O_3$ to HOx was only <2%. Compared with our result, the daily HCHO concentrations in Milan and Beijing were usually higher than 15 ppb [*Alicke et al.*, 2002; *An et al.*, 2009], and HCHO became the most important source (>45%) for HOx radicals. The HCHO level in NYC is much lower than those in Milan and Beijing, only 2.2 ppb on average in this study. As a result, its contribution to HOx was less than that of HONO.

4. Summary and Conclusions

[24] Ambient HCHO measurements were obtained from 16 July to 3 August in 2009 using QC laser spectroscopy in NYC. This study investigates the characteristics, sources of ambient HCHO and its contribution to HOx free radicals during the summertime. During the sampling period, the average HCHO concentration was 2.2 ± 1.1 ppb. The daily maximum concentration was usually found at noontime, while the minimum value was observed during the pre-dawn morning hours. Correlation analyses showed that HCHO correlated strongly with NOx and BC during the morning rush hour, while it correlated better with total oxidants (Ox) between 1100 EST and 1400 EST. This indicates that both primary and secondary sources contributed to ambient HCHO in this mega-city. The primary and secondary HCHO concentrations were estimated according to the HCHO/BC ratios. Secondary HCHO was estimated to be as high as 70% of the HCHO concentration between 1200 EST and 1500 EST. Isoprene was the most important source of secondary HCHO, accounting for about 44%, followed by methane (25%) and propene (18%). However, ethylene is also an important precursor of secondary HCHO, but it was not considered in this study since it was not measured. Finally, we also assessed the HOx production rate in this study. The rate averaged 1.3×10^7 molecules cm^3/s with maximum value of 2.4×10^7 observed at 11 EST, with HONO, HCHO and O_3 responsible for 67, 18 and 13% of HOx radical formation.

[25] **Acknowledgments.** This field study was supported by NYSERDA contract 10602. Purchase and outfitting of the mobile laboratory was made possibly by support from NYSTAR, the New York State Office of Science, Technology and Academic Research (contract #3538479). We acknowledge the help and support of New York State Department of Environmental Conservation in making this study possible, and helping with its execution. We also thank Queens College for hosting the field study and acknowledge our Aerodyne Research Inc. partners.

References

Alicke, B., U. Platt, and J. Stutz (2002), Impact of nitrous acid photolysis on the total hydroxyl radical budget during the Limitation of Oxidant Production/Pianura Padana Produzion di Ozono study in Milan, *J. Geophys. Res.*, *107*(D22), 8196, doi:10.1029/2000JD000075.

An, J., W. Zhang, and Y. Qu (2009), Impact of a strong cold front on concentrations of HONO, HCHO, O_3, and NO_2 in an heavy traffic urban area of Beijing, *Atmos. Environ.*, *43*, 3454–3459, doi:10.1016/j.atmosenv.2009.04.052.

Anderson, L. G., J. A. Lanning, R. Barrell, J. Miyagishima, R. H. Jones, and P. Wolfe (1996), Source and sinks of formaldehyde and acetaldehyde: An analysis of Denver's ambient concentration data, *Atmos. Environ.*, *30*, 2113–2123, doi:10.1016/1352-2310(95)00175-1.

Apel, E. C., et al. (1998), Measurements comparison of oxygenated volatile organic compounds at a rural site during the 1995 SOS Nashville Intensive, *J. Geophys. Res.*, *103*, 22,295–22,316, doi:10.1029/98JD01753.

Apel, E. C., et al. (2008), Intercomparison of oxygenated volatile organic compound measurements at the SAPHIR atmosphere simulation chamber, *J. Geophys. Res.*, *113*, D20307, doi:10.1029/2008JD009865.

Atkinson, R. (1997), Gas-phase tropospheric chemistry of volatile organic compounds. 1. Alkanes and alkenes, *J. Phys. Chem. Ref. Data*, *26*, 215–290, doi:10.1063/1.556012.

Ban-Weiss, G. A., J. P. McLaughlin, R. A. Harley, M. M. Lunden, T. W. Kirchstetter, A. J. Kean, A. W. Strawa, E. D. Stevenson, and G. R. Kendall (2008), Long-term changes in emissions of nitrogen oxides and particulate matter from on-road gasoline and diesel vehicles, *Atmos. Environ.*, *42*, 220–232, doi:10.1016/j.atmosenv.2007.09.049.

Buzcu Guven, B., and E. P. Olaguer (2011), Ambient formaldehyde source attribution in Houston during TexAQS II and TRAMP, *Atmos. Environ.*, *45*, 4272–4280, doi:10.1016/j.atmosenv.2011.04.079.

Cárdenas, L. M., D. J. Brassington, B. J. Allan, H. Coe, B. Alicke, U. Platt, K. M. Wilson, J. M. C. Plane, and S. A. Penkett (2000), Intercomparison of formaldehyde measurements in clean and polluted atmospheres, *J. Atmos. Chem.*, *37*, 53–80, doi:10.1023/A:1006383520819.

Chen, J., S. So, H. Lee, M. P. Fraser, R. F. Curl, T. Harman, and F. K. Tittel (2004), Atmospheric formaldehyde monitoring in the greater Houston Area 2002, *Appl. Spectrosc.*, *58*, 243–247, doi:10.1366/000370204322843002.

Dasgupta, P. K., J. Li, G. Zhang, W. T. Luke, W. A. McClenny, J. Stutz, and A. Fried (2005), Summertime ambient formaldehyde in five U.S. metropolitan areas: Nashville, Atlanta, Houston, Philadelphia, and Tampa, *Environ. Sci. Technol.*, *39*, 4767–4783, doi:10.1021/es048327d.

Dong, S., and P. K. Dasgupta (1987), Fast fluorometric flow injection analysis of formaldehyde in atmospheric water, *Environ. Sci. Technol.*, *21*, 581–588, doi:10.1021/es00160a009.

Elshorbany, Y. F., R. Kurtenbach, P. Wiesen, F. Lissi, M. Rubio, G. Villena, E. Gramsch, A. R. Rickard, M. J. Pilling, and J. Kleffmann (2009), Oxidation capacity of the city air of Santiago, Chile, *Atmos. Chem. Phys.*, *9*, 2257–2273, doi:10.5194/acp-9-2257-2009.

Fan, Q., and P. K. Dasgupta (1994), Continuous automated determination of atmospheric formaldehyde at the parts per trillion levels, *Anal. Chem.*, *66*, 551–556, doi:10.1021/ac00076a021.

Fischer, H., et al. (1998), Trace gas measurements during the Oxidizing Capacity of the Tropospheric Atmosphere campaign 1993 at Izana, *J. Geophys. Res.*, *103*, 13,505–13,518, doi:10.1029/97JD01497.

Fried, A., Y.-N. Lee, G. Frost, B. Wert, B. Henry, J. R. Drummond, G. Huebler, and T. Jobson (2002), Airborne CH_2O Measurements over the North Atlantic during the 1997 NARE Campaign: Instrument comparisons and distributions, *J. Geophys. Res.*, *107*(D4), 4039, doi:10.1029/2000JD000260.

Fried, A., et al. (2003), Tunable diode laser measurements of formaldehyde during the TOPSE 2000 study: Distribution, trends, and model comparisons, *J. Geophys. Res.*, *108*(D4), 8365, doi:10.1029/2002JD002208.

Garcia, A. R., R. Volkamer, L. T. Molina, M. J. Molina, J. Samuelson, J. Mellqvist, B. Galle, S. C. Herndon, and C. E. Kolb (2006), Separation of emitted and photochemical formaldehyde in Mexico City using a statistical analysis and a new pair of gas-phase tracers, *Atmos. Chem. Phys.*, *6*, 4545–4557, doi:10.5194/acp-6-4545-2006.

Gilpin, T., et al. (1997), Intercomparison of Six Ambient [CH_2O] Measurement Techniques, *J. Geophys. Res.*, *102*, 21,161–21,188, doi:10.1029/97JD01314.

Grutter, M., E. Flores, G. Anadraca-Ayala, and A. Baez (2005), Formaldehyde levels in downtown Mexico City during 2003, *Atmos. Environ.*, *39*, 1027–1034, doi:10.1016/j.atmosenv.2004.10.031.

Hak, C., et al. (2005), Intercomparison of four different in-situ techniques for ambient formaldehyde measurements in urban air, *Atmos. Chem. Phys.*, *5*, 2881–2900, doi:10.5194/acp-5-2881-2005.

Harder, J. W., A. Fried, S. Sewell, and B. Henry (1997), Comparison of tunable diode laser and long-path ultraviolet/visible spectroscopic measurements of ambient formaldehyde concentrations during the 1993 OH photochemistry experiments, *J. Geophys. Res.*, *102*, 6267–6282, doi:10.1029/96JD01731.

Harley, R. A., and G. R. Cass (1994), Modeling the concentrations of gas-phase toxic organic air pollutants: Direct emissions and atmospheric formation, *Environ. Sci. Technol.*, *28*, 88–98, doi:10.1021/es00050a013.

Heikes, B., et al. (1996), Formaldehyde methods comparison in the remote lower troposphere during the Mauna Loa Photochemistry Experiment 2, *J. Geophys. Res.*, *101*, 14,741–14,755, doi:10.1029/96JD00550.

Herndon, S. C., J. H. Shorter, M. S. Zahniser, J. Wormhoudt, D. D. Nelson, K. L. Demerjian, and C. E. Kolb (2005), Real-time measurements of SO_2, H_2CO, and CH_4 emissions from in-use curbside passenger buses in New York City using a chase vehicle, *Environ. Sci. Technol.*, *39*, 7984–7990, doi:10.1021/es0482942.

Herndon, S. C., M. S. Zahniser, D. D. Nelson Jr., J. Shorter, J. B. McManus, R. Jiménez, C. Warneke, and J. A. de Gouw (2007), Airborne measurements of HCHO and HCOOH during the New England Air Quality Study using a pulse quantum cascade laser spectrometer, *J. Geophys. Res.*, *112*, D10S03, doi:10.1029/2006JD007600.

Hottle, J. R., A. J. Huisman, J. P. Digangi, A. Kammrath, M. M. Galloway, K. L. Coens, and F. N. Keutsch (2009), A laser induced fluorescence-based instrument for in-situ measurements of atmospheric formaldehyde, *Environ. Sci. Technol.*, *43*, 790–795, doi:10.1021/es801621f.

Jiang, M., et al. (2005), Vehicle fleet emissions of black carbon, polycyclic aromatic hydrocarbons, and other pollutants measured by a mobile laboratory in Mexico City, *Atmos. Chem. Phys.*, *5*, 3377–3387, doi:10.5194/acp-5-3377-2005.

Kolb, C., S. C. Herndon, J. B. McManus, J. H. Shorter, M. S. Zahniser, D. D. Nelson, J. T. Jayne, M. R. Canagaratna, and D. R. Worsnop (2004), Mobile laboratory with rapid response instruments for real-time measurements of urban and regional trace gas and particulate distributions and emission source characteristics, *Environ. Sci. Technol.*, *38*, 5694–5703, doi:10.1021/es030718p.

Lawson, D. R., H. W. Biermann, E. C. Tuazon, A. M. Winer, G. I. Mackay, H. I. Schiff, G. L. Kok, P. K. Dasgupta, and K. Fung (1990), Formaldehyde measurement methods evaluation and ambient concentrations during the Carbonaceous Species Method Comparison Study, *Aerosol Sci. Technol.*, *12*, 64–76, doi:10.1080/02786829008959326.

Lazrus, A. L., K. L. Fong, and J. A. Lind (1988), Automatic fluorometric determination of formaldehyde in air, *Anal. Chem.*, *60*, 1074–1078, doi:10.1021/ac00161a025.

Lee, Y. N., et al. (1998), Atmospheric chemistry and distribution of formaldehyde and several multioxygenated carbonyl compounds during 1995 Nashville/Middle Tennessee Ozone Study, *J. Geophys. Res.*, *103*, 22,449–22,462, doi:10.1029/98JD01251.

Li, Y. Q., K. L. Demerjian, M. S. Zahniser, D. D. Nelson, J. B. McManus, and S. C. Herndon (2004), Measurement of formaldehyde, nitrogen dioxide, and sulfur dioxide at Whiteface Mountain using a dual tunable diode laser system, *J. Geophys. Res.*, *109*, D16S08, doi:10.1029/2003JD004091.

Li, Y., M. Shao, S. H. Lu, C.-C. Chang, and P. K. Dasgupta (2010), Variations and sources of ambient formaldehyde for the 2008 Beijing Olympic games, *Atmos. Environ.*, *44*, 2632–2639, doi:10.1016/j.atmosenv.2010.03.045.

Macdonald, A. M., P. A. Markar, K. G. Anlauf, K. L. Hayden, J. W. Bottenheim, D. Wang, and T. Dann (2001), Summertime formaldehyde at a high-elevation site in Quebec, *J. Geophys. Res.*, *106*, 32,361–32,374, doi:10.1029/2001JD000513.

Mackay, G. I., D. R. Karecki, and H. I. Schiff (1996), Tunable diode laser absorption measurements of H_2O_2 and HCHO during the Mauna Loa Observatory Photochemistry Experiment, *J. Geophys. Res.*, *101*, 14,721–14,728, doi:10.1029/95JD03655.

Nelson, D. D., J. H. Shorter, J. B. McManus, and M. S. Zahniser (2002), Sub-part-per-billion detection of nitric oxide in air using a thermoelectrically cooled mid-infrared quantum cascade laser spectrometer, *Appl. Phys. B*, *75*, 343–350, doi:10.1007/s00340-002-0979-4.

Oliver, K., J. R. Adams, E. H. Daughtrey Jr., W. A. McClenny, M. J. Yoong, and M. A. Pardee (1996), Technique for monitoring ozone precursor hydrocarbons in air at photochemical assessment monitoring stations: Sorbent preconcentration, closed-cycle cooler cryofocusing, and GC-FID analysis, *Atmos. Environ.*, *30*, 2751–2757, doi:10.1016/1352-2310(95)00371-1.

Parrish, D. D., and F. C. Fehsenfeld (2000), Methods for gas-phase measurements of ozone, ozone precursors and aerosol precursors, *Atmos. Environ.*, *34*, 1921–1957, doi:10.1016/S1352-2310(99)00454-9.

Paulson, S. E., M. Y. Chung, and A. S. Hasson (1999), OH radical formation from the gas-phase reaction of ozone and the relationship between structure and mechanism, *J. Phys. Chem.*, *103*, 8125–8138.

Possanzini, M., V. Di Palo, and A. Cecinato (2002), Sources and photodecomposition of formaldehyde and acetaldehyde in Rome ambient air, *Atmos. Environ.*, *36*, 3195–3201, doi:10.1016/S1352-2310(02)00192-9.

Rappenglück, B., P. K. Dasgupta, M. Leuchner, Q. Li, and W. Luke (2010), Formaldehyde and its relation to CO, PAN, and SO_2 in the Houston-Galveston airshed, *Atmos. Chem. Phys.*, *10*, 2413–2424, doi:10.5194/acp-10-2413-2010.

Ren, X., H. Harder, M. Martinez, R. L. Lesher, A. Oliger, T. Shirley, J. Adams, J. B. Simpas, and W. H. Brune (2003a), HOx concentrations and OH reactivity observations in New York City during PMTACS-NY2001, *Atmos. Environ.*, *37*, 3627–3637, doi:10.1016/S1352-2310(03)00460-6.

Ren, X., et al. (2003b), OH and HO_2 chemistry in the urban atmosphere of New York City, *Atmos. Environ.*, *37*, 3639–3651, doi:10.1016/S1352-2310(03)00459-X.

Rothman, L. S., et al. (1998), The HITRAN molecular spectroscopic database and Hawks (HITRAN Atmospheric Workstation): 1996 Edition, *J. Quant. Spectrosc. Radiat. Transfer*, *60*, 665–710, doi:10.1016/S0022-4073(98)00078-8.

Satsumabayashi, H., H. Kurita, Y.-S. Chang, and G. R. Carmichael (1995), Photochemical formations of lower aldehydes and lower fatty acids under long-range transport in central Japan, *Atmos. Environ.*, *29*, 255–266, doi:10.1016/1352-2310(94)00231-9.

Schauer, J. J., M. J. Kleeman, G. R. Cass, and B. R. T. Simoneit (2002), Measurement of emissions from air pollution sources. 5. C1–C32 organic compounds from gasoline-powered motor vehicles, *Environ. Sci. Technol.*, *36*, 1169–1180, doi:10.1021/es0108077.

Schwab, J. J., Y. Li, and K. L. Demerjian (2004), Semi-continuous formaldehyde measurements with a diffusion scrubber/liquid fluorescence analyzer, paper presented at Symposium on Air Quality Measurement Methods and Technology-2004, Air and Waste Manage. Assoc., Pittsburgh, Pa.

Schwab, J. J., M.-S. Bae, G. G. Lala, K. L. Demerjian, W.-N. Chen, Y. C. Lin, Y. Sun, and Q. Zhang (2010), A mobile laboratory for on-road and near-roadway measurements of fine particulate matter and pollutant gases, paper presented at 2010 Specialty Conference, AAAR, San Diego, Calif.

Seinfeld, J. H., and S. N. Pandis (1998), *Atmospheric Chemistry and Physics: From Air Pollution to Climate Change*, John Wiley, Hoboken, N. J.

Slemr, J., W. Junkermann, and A. Votz-Thomas (1996), Temporal variations in formaldehyde, acetaldehyde and acetone and budget of formaldehyde at a rural site in southern Germany, *Atmos. Environ.*, *30*, 3667–3676, doi:10.1016/1352-2310(96)00025-8.

Sprengnether, M., K. L. Demerjian, N. M. Donahue, and J. G. Anderson (2002), Product analysis of the OH oxidation of isoprene and 1,3-butandine in the presence of NO, *J. Geophys. Res.*, *107*(D15), 4268, doi:10.1029/2001JD000716.

Sumner, A. L., et al. (2001), A study of formaldehyde chemistry above a forest canopy, *J. Geophys. Res.*, *106*, 24,387–24,405, doi:10.1029/2000JD900761.

Sun, Y., et al. (2011), Characterization of the source and process of organic and inorganic aerosols in New York City with a high-resolution time-of-flight aerosol mass spectrometer, *Atmos. Chem. Phys.*, *11*, 1581–1602, doi:10.5194/acp-11-1581-2011.

Sun, Y. L., et al. (2012), Characterization of near-highway submicron aerosols in New York City with a high-resolution aerosol mass spectrometer, *Atmos. Chem. Phys.*, *12*, 2215–2227, doi:10.5194/acp-12-2215-2012.

Venkatachari, P., L. Zhou, P. K. Hopke, D. Felton, O. V. Rattigan, J. J. Schwab, and K. L. Demerjian (2006), Spatial and temporal variability of black carbon in New York City, *J. Geophys. Res.*, *111*, D10S05, doi:10.1029/2005JD006314.

von Schneidemesser, E., P. S. Monks, and C. Plass-Duelmer (2010), Global comparison of VOC and CO observations in urban areas, *Atmos. Environ.*, *44*, 5053–5064, doi:10.1016/j.atmosenv.2010.09.010.

Wang, X., H. Wang, and S. Wang (2010), Ambient formaldehyde and its contributing factor to ozone and OH radical in rural area, *Atmos. Environ.*, *44*, 2074–2078, doi:10.1016/j.atmosenv.2010.03.023.

Wert, B. P., et al. (2003), Signatures of terminal alkene oxidation in airborne formaldehyde measurements during TexAQS 2000, *J. Geophys. Res.*, *108*(D3), 4104, doi:10.1029/2002JD002502.

Wisthaler, A., et al. (2008), Technical note: Intercomparison of formaldehyde measurements at the atmosphere simulation chamber SAPHIR, *Atmos. Chem. Phys.*, *8*, 2189–2200, doi:10.5194/acp-8-2189-2008.

Zhang, Q., et al. (2007), Ubiquity and dominance of oxygenated species in organic aerosols in anthropogenically influenced Northern Hemisphere midlatitudes, *Geophys. Res. Lett.*, *34*, L13801, doi:10.1029/2007GL029979.

Zhou, X., Y.-N. Lee, L. Newman, X. Chen, and K. Mopper (1996), Tropospheric formaldehyde concentration at the Mauna Loa Observatory during MLOPEX II, *J. Geophys. Res.*, *101*, 14,711–14,719, doi:10.1029/95JD03226.

Zhou, X., Y. He, J. Hou, H. Gao, J. J. Schwab, X. Ren, and W. H. Brune (2004), Atmospheric chemistry of HONO and HNO_3: Their impact on air quality in urban environments. paper presented at International Conference on the Urban Dimensions of Environmental Change: Science, Exposures, Policies, and Technologies, Urban Dimensions of Environ. Change Conf. Comm., Shanghai, China.

Zhou, X., G. Huang, K. Civerolo, U. Roychowdhury, and K. L. Demerijian (2007), Summertime observations of HONO, HCHO, and O_3 at the summit of Whiteface Mountain, New York, *J. Geophys. Res.*, *112*, D08311, doi:10.1029/2006JD007256.

M.-S. Bae, Department of Environmental Engineering, Mokpo National University, Muan, Jeollanamdo 534-729, South Korea.

W.-N. Chen and Y. C. Lin, Research Center for Environmental Changes, Academia Sinica, 128 Academia Rd., Section 2, Nankang, Taipei 115, Taiwan. (yclin26@rcec.sinica.edu.tw)

K. L. Demerjian and J. J. Schwab, Atmospheric Sciences Research Center, State University of New York at Albany, 251 Fuller Rd., Albany, NY 12203, USA.

H.-M. Hung, Department of Atmospheric Sciences, National Taiwan University, Taipei 106, Taiwan.

J. Perry, New York State Department of Environmental Conservation, Albany, NY 12233, USA.

Y. Sun, State Key Laboratory of Atmospheric Boundary Layer Physics and Atmospheric Chemistry, Institute of Atmospheric Physics, Chinese Academy of Sciences, Beijing 100029, China.

Q. Zhang, Department of Environmental Toxicology, University of California, Davis, CA 95616, USA.